RPE | Radiation Physics & Engineering
A Peer-Reviewed Journal
Published by K.N. Toosi University of Technology
http://rpe.kntu.ac.ir
Research Article

Radiation Physics and Engineering 2025; 6(3):1–8

Dosimetry and analysis of the delayed gamma rays emitted from the irradiated holder device used in Mo-99 production facilities

Seyed Milad Miremad*, Ali Bahrami-Samani, Mohsen Tabasi, Mohammad Ghannadi-Maragheh
Nuclear Science and Technology Research Institute (NSTRI), P.O. Box: 14395-836, Tehran, Iran

HIGHLIGHTS

- The holder material indirectly affects the activity of Mo-99 produced in LEU targets.
- The proposed method is reliable for the estimation of the gamma-ray spectrum.
- The dose rate of irradiated Al-Alloy 6061 holder device decreases faster.
- A container with 22 cm lead walls is suitable for holder batch transportations.

ABSTRACT

The vital radioisotope ^{99m}Tc, used in approximately 80-85% of diagnostic radiopharmaceuticals, is mostly obtained from the decay of Mo-99. To provide 100 Ci Mo-99 (6 days) per week for Iran's domestic nuclear medicine centers, an industrial plan of Mo-99 production via fission of Low Enrichment Uranium targets in the Tehran Research Reactor has recently been evaluated. In this regard and with the aim of better conceptual knowledge for the site's solid waste management, two holders made of Al-Alloy 6061 and Stainless Steel-316, which will be used to irradiate the targets, were investigated in this paper. The gamma spectrum emitted from the irradiated holder device and the corresponding dose rate were calculated by a proposed method that had been verified experimentally. When the Al-Alloy 6061 holder device was used, the calculation results indicated that the Mo-99 activity produced in the mini-plates was higher and the gamma dose rate of the activated holder device decreased faster.

KEYWORDS

Dosimetry
Gamma spectroscopy
Mo-99 production
Tehran research reactor
Solid waste management
MCNPX

HISTORY

Received: 26 August 2024
Revised: 14 October 2024
Accepted: 13 December 2024
Published: Summer 2025

1 Introduction

Technetium-99m has been widely used in clinical nuclear imaging procedures for diagnosing cancer and heart diseases. ^{99m}Tc is approximately used in 80-85% of all nuclear medicine procedures in the world (Domingos et al., 2011; Hasan and Prelas, 2020). This vital isotope is obtained from its parent decay Mo-99. ^{98}Mo$(n,\gamma)^{99}$Mo interaction and fission of U-235 are two different approaches for Mo-99 production by research reactors. Although the fission method is complex and expensive, it has the highest efficiency for Mo-99 production (Lee et al., 2016, 2020; Muenze et al., 2013; Park et al., 2000). The internal consumption of Mo-99 has been estimated approximately at about 100 Ci (6 days) every week, in the Islamic Republic of Iran. Accordingly, an industrial evaluation for Mo-99 production via fission of Low Enrichment Uranium (LEU) targets in the Tehran Research Reactor (TRR) is performing. For this purpose, a specific type of domestic mini plates was designed as LEU targets. Their U-235 enrichment is equal to 19.7% with a tolerance of ±0.2%. The meat combination (U_3O_8) has been covered by a thin Aluminum clad. Each mini plate contains 2.6 g U-235 and its dimensions are $20 \times 5.1 \times 0.15$ cm^3.

To load the mini plates inside the TRR core, an industrial holder device was designed. After irradiation in the TRR core, the holder batch (including 10 irradiated mini plates) is transported to the Hot Cell Complex (HCC) by a suitable container for beginning the radiochemical process of the mini plates. After removing the irradiated mini plates, it is dangerous to extract the empty holder device from HCC due to its high activity. After a few days, the new fresh mini plates will be loaded in the decayed holder device, inside the HCC, and the prepared holder batch will be transferred to the reactor site for new irradiation. To handle the holder device, its gamma lines

*Corresponding author: smmiremad@aeoi.org.ir

https://doi.org/10.22034/rpe.2024.475273.1238

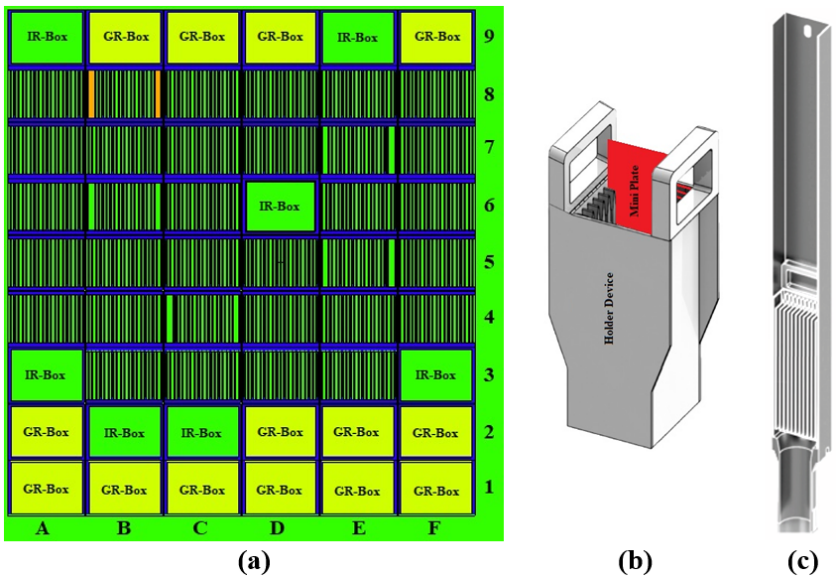

Figure 1: a) The core of TRR simulated by MCNPX code b) Holder device structure c) Position of holder batch in the D6 channel of TRR core.

spectrum and corresponding dose rate must be estimated under various conditions. For example, if the Mo-99 production facility is closed after occurring an accident, the active holders must remain in the HCC or a place with adequate shielding walls for a reasonable decay-delay period until their dose rates are reduced to the permissible limits. Simulation studies could be useful for characterizing the delayed gamma-rays emitted from neutron-activated holder batches. To estimate the accurate gamma dose rates and handle the activated holder devices (including transport, storage, shielding, etc.), meticulous calculations are needed. Delayed particle emission has been implemented since Monte Carlo N-Particle code (MCNPX) version 2.6.c (McKinney et al., 2007). The delayed gamma code in MCNPX has not substantially been improved in its next release version, one issue being that the code wastes a lot of memory and computer time (De Stefano et al., 2020). In addition, incorrect gamma peaks appear when MCNPX is run with full discrete data, and sometimes some correct peaks disappear in the result (Lou and Ludewigt, 2015). This paper describes a multi-step method for calculating the spectrum of delayed gamma-rays emitted from the irradiated holder batches. Two types of holder devices made of Al-Alloy 6061 (AA6061) and Stainless Steel 316 (SS316) have been investigated. Validation of the method was evaluated experimentally using some samples of both materials. After verifying, the proposed method was used to estimate the holder device dose rate in some conditions.

2 Materials and Methods

2.1 Tehran Research Reactor

TRR is a 5 MW thermal power research reactor used for medicine and industrial radioisotope production, neutron activation analysis, etc. TRR core includes 6×9 boxes to mount various types of core components such as fuel elements (Standard Fuel Elements (SFE) and Control Fuel Elements (CFE)), IR-Boxes (for samples irradiation purposes) and GR-Boxes (graphite blocks as the core reflector). The recently used core configuration consists of 28 SFEs and 5 CFEs. SFE has 19 fuel plates while CFE has 14 fuel plates (Abedi et al., 2016; Hedayat et al., 2021). Figure 1-a shows the MCNPX-2.7.e simulation of TRR core configuration which has been used in the proposed calculation method of the present study.

2.2 Sample Plates and Holder Device

A holder device has been designed to load 10 fresh mini plates inside the core. The structure of the holder device and the position of the holder batch in the D6 channel during irradiation are shown in Figs. 1-b and 1-c, respectively. The holder could be made by nuclear grade AA6061 or SS316. For experimentally evaluations several prototype rectangular samples with dimensions $0.15 \times 4 \times 10$ cm^3 of both materials were prepared to irradiate in the center of the D6 channel of the TRR core.

3 Experimental

Five samples of each material were irradiated at the center of the D6 channel, separately. The average power of TRR and approximate irradiation time were 2 MW and 5 min, respectively. After irradiation, the samples were held in a radiation safe container. They were examined at the end of each decay-delay time from 1 to 6 days. The dose rates of samples were measured by the RDS-31 detector. RDS-31 is a small handheld survey instrument utilizing an energy-compensated GM-tube as a primary detector. For each dosimetry setup, the RDS-31 detector's dose rate was recorded after 1 minute, repeated 5 times, and the mean values and relative errors of these measurements were reported. In addition, an HPGe detector was used to measure the gamma rays spectrum emitted from each sample. The gamma-rays detector system consisted of a detector

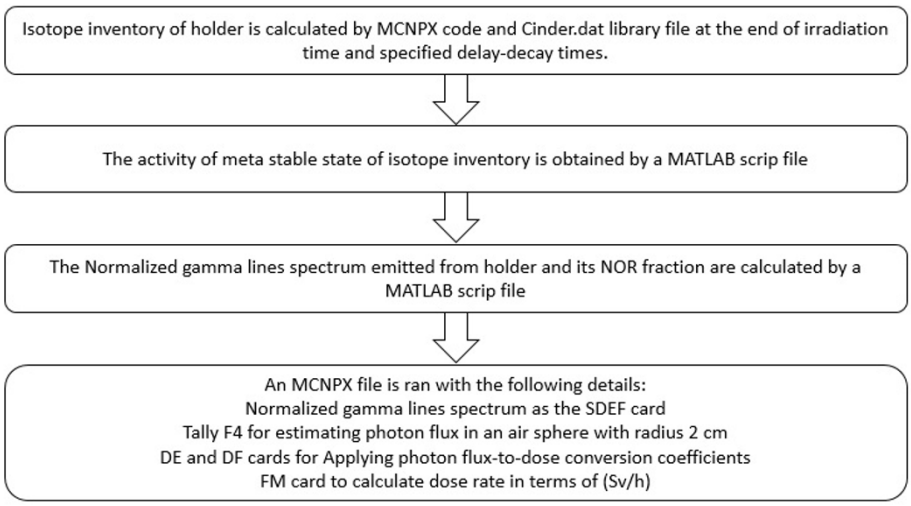

Figure 2: Flow chart of the proposed method for calculation of delayed gamma rays and corresponding dose rate.

Table 1: Holder isotopes inventory at the time (t).

Isotope number	Activity (Ci)	Emitted gamma rays properties		
		Number	Energy (MeV)	Abundance
1	A_1	i	E_{11}, E_{12}, ..., E_{1i}	F_{11}, F_{12}, ..., F_{1i}
2	A_2	j	E_{21}, E_{22}, ..., E_{2j}	F_{21}, F_{22}, ..., F_{2j}
⋮	⋮	⋮	⋮	⋮
N	A_N	z	E_{N1}, E_{N2}, ..., E_{Nz}	F_{N1}, F_{N2}, ..., F_{Nz}

Table 2: The calculated spectrum of delayed gamma rays emitted from the holder isotope inventory.

The gamma line energy (MeV)	Related abundance
E_{11}, ..., E_{1i}	$\frac{A_1F_{11}}{NOR}$, ..., $\frac{A_1F_{1i}}{NOR}$
E_{21}, ..., E_{2i}	$\frac{A_2F_{21}}{NOR}$, ..., $\frac{A_2F_{2j}}{NOR}$
⋮	⋮
E_{N1}, ..., E_{Nz}	$\frac{A_NF_{N1}}{NOR}$, ..., $\frac{A_NF_{Nz}}{NOR}$

bias supply, preamplifier, amplifier, analog-to-digital converter (ADC), multichannel analyzer (MCA), computer and spectrum analysis software. In this case, the gamma count was recorded for 5 min. The FWHM of calibrated HPGe detector system was about 2.5 keV for the 1.33 MeV gamma-ray of Co-60. This FWHM is sufficient for the detection and separation of most radioisotopes.

4 Calculation

Delayed gamma rays can be calculated by the ACT card in the MCNPX2.7e code. When the DG keyword is equal to LINES, it performs analog sampling of delayed gammas using models based on line-emission data (which is currently available for 979 nuclides) augmented by 25-group data (available for the other 3400 nuclides in the CINDER90 database). Running the program with this card is time-consuming and it also requires a lot of memory. In addition, studies show that the dose rate has a large error when it is calculated by the spectrum which was obtained by the ACT card. To put it another way, sometimes this spectrum has some high energy gamma rays that cannot be attributed to any isotope of the activated sample inventory. So a more valid method was proposed to calculate delayed gamma rays. The flow chart of the proposed method for delayed gamma rays calculation and corresponding dose rate is shown in Fig. 2. At first, the activity of the actinide and non-actinide inventory of the irradiated holder batch was calculated by MCNPX. The inventory includes actinides, fission products, activation products, and all isotopes that exist in their decay series. The depletion/burnup capability (Burn card) was used. It has been limited by criticality (KCODE) problems and needs the CINDER.dat library file to calculate depletion properly. CINDER.dat library file contains decay, fission yield, and 63-group cross-section data not calculated by MCNPX. Except for fission products of burnup Tier3, the interest isotopes were added to the material card (M) by providing appropriate isotope identifiers with 10^{36} atomic/weight fraction.

The time steps in the Burn card were small enough to capture the flux-shape change accurately over time. A

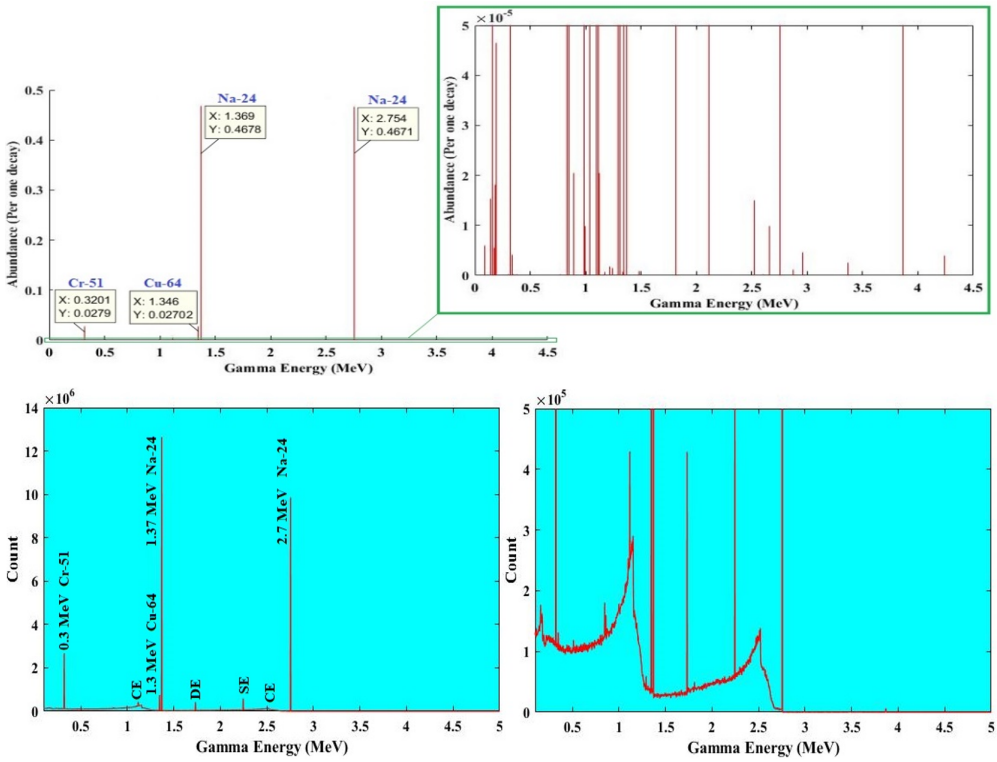

Figure 3: Calculated gamma line spectrum (top) and recorded gamma spectrum by HPGe (down) for AA6061 sample No. 3.

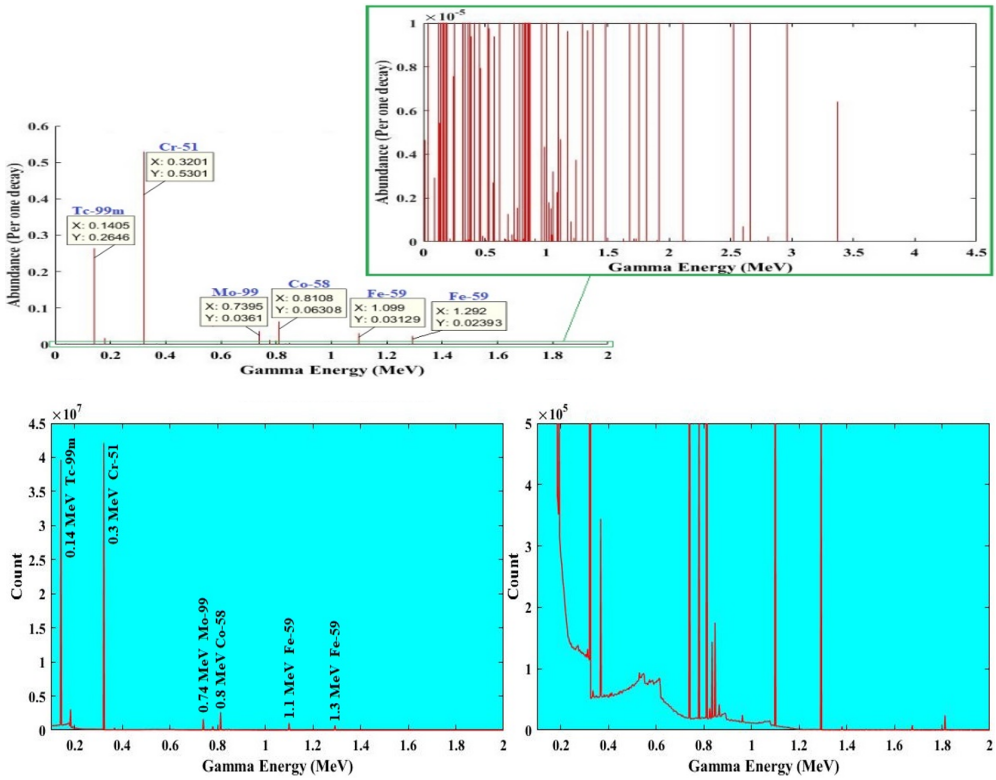

Figure 4: Calculated gamma line spectrum (top) and recorded gamma spectrum by HPGe (down) for SS316 sample No. 3.

high-speed cluster computer was used in this step. The activities of the metastable states of radioisotopes are not shown in the MCNPX output files (such as ^{99m}Tc in the decay chain of Mo-99). So in step 2, the activities of these isotopes were calculated by a MATLAB script file which is written based on decay chain properties of isotopes inventory. Each radioisotope emits one or more gamma rays in one decay. According to Eq. (1), the total gamma dose

rate depends on the activities of radioisotopes and their gamma emission properties (such as the number of emitted gamma rays, their energies, and related abundances). The holder inventory changes with time, and for a specific moment, the inventory is shown in Table 1.

$$D_1 \propto \Big[(A_1 \times \sum_{1}^{i} E_{1i} \times F_{1i}) + (A_2 \times \sum_{1}^{j} E_{2j} \times F_{2j}) + \cdots + (A_N \times \sum_{1}^{z} E_{Nz} \times F_{Nz})\Big] \quad (1)$$

The gamma lines spectrum extracted from Eq. (1) can be used for calculating the gamma dose rate in any form of geometry. The calculated spectrum is shown in Table 2. The NOR is a constant which is obtained from Eq. (2).

$$NOR = \Big[(\sum_{1}^{i} A_1 F_{1i}) + (\sum_{1}^{j} A_2 F_{2j}) + \cdots + (\sum_{1}^{z} A_N F_{Nz})\Big] \quad (2)$$

The gamma line spectrum was calculated based on the data obtained from the ENDF-VIII.B library of JANIS software, in step 3. At the end step, the suitable geometry will be drawn in the MCNPX input file and finally, the gamma dose rate will be calculated according to photon flux-to-dose conversion coefficients of AP geometry in the ANSI/ANS-6.1.1-2020 standard. The Stop card was used in MCNPX input files to stop calculations when the fluctuation chart of tally has a relative error less than 0.05. So the qualities of tallies are reliable.

5 Results

5.1 Validation of Proposed Method

Seven IR-boxes exist in the selected core configuration. Both simulation results and practical observations during reactor operation showed that the D6 channel has the highest neutron flux among all IR-boxes.

In D6 channel, the average neutron flux with the energy range of 0-0.625 eV in the situation of target irradiation was calculated at about 5×10^{13} n.cm^{-2}.s^{-1}. Table 3 shows the average weight of each element in AA6061 and SS316 obtained from (McConn et al., 2011). According to the isotopic abundance of each element, the weight fraction of their isotopes was calculated. The measured and calculated dose rate at a distance of 50 cm away from the larger surface of the AA6061 and SS316 samples are shown in Table 4.

Besides, the gamma spectrum of samples was recorded by an HPGe detector. The background gamma was subtracted from the measured spectrum to obtain the gamma rays spectrum emitted from the sample only. For instance, the gamma spectrum of the 3rd sample of both materials and their gamma calculated lines spectrum, after 2 days delay-decay are depicted in Figs. 3 and 4.

5.2 Holder Device Handling

The irradiation of the holder device with 10 fresh mini plates was simulated by MCNPX. It was assumed that the reactor operates with maximum thermal power (5 MW) with 80% control rods off, in the irradiation period (6 days). The calculated neutronic safety parameters of the TRR core after loading the holder batch in the bottom of the D6 channel showed that safety limits are fulfilled in both cases. After 1 day, the cooled holder batch is transported to HC1 by a container. The gamma dose rates on the surface of some symmetrical containers are shown in Table 5. The containers have stainless steel framework which is filled with lead material.

In the HCC, ten mini plates remove from the holder for radiochemical processing. The gamma dose rates on the surface of the empty activated holder are shown in Table 6.

6 Discussion

RDS-31 can detect gamma and X-rays from 48 keV to 3 MeV. Its energy response is accorded to ambient dose equivalent H*(10) and its dose rate measurement range is 0.01 μSv.h^{-1} to 0.1 Sv.h^{-1}. The background dose rate was 0.14 μSv.h^{-1} in the laboratory layout which was subtracted from the measured values. The ambient dose equivalent measured with a survey meter is defined as the dose equivalent at a depth of 1 cm from the surface of an ICRU sphere that is 30 cm in diameter. In comparison, according to the ANSI-6.1.1 standard, the effective dose will be obtained by applying conversion coefficients. With this in mind, it makes perfect sense for the ambient dose equivalent measured with RDS-31 to be larger than the calculated effective dose. It should be noted that considering a distance of 50 cm for measurement can greatly reduce the effect of beta particles emitted from samples. For a short delay-decay period, the deviations of the RDS-31 measurements were greater. After a longer one, these deviations were reduced and the differences between the measured and calculated dose rate values were also decreased. It is because for a long delay-decay period, the short-lived radioisotopes are eliminated and the holder inventory will become more stable. The background-less gamma spectrum includes Compton Edge (CE), Single Escape (SE), Double Scape (DE), and photopeak of gamma lines. As can be seen, the radioisotopes estimated from the measured spectrum correspond to the calculated inventory of the samples.

What's more, it is observed that the ratio of two selected photopeak areas in the measured spectrum differs from the ratio of their abundances in the calculated spectrum. This is derived from the energy response function of the detector system which is related to some parameters like the attenuation effect of Be window, the interaction probability of photon with Ge material, and so on. For example, Na-24 which is produced in the irradiated AA6061 sample will be recognized from two dominant gamma-rays 1.37 and 2.75 MeV. The photopeak areas of these energies were 3.15×10^4 and 2.46×10^4 Count. MeV,

Table 3: Isotope characteristic of holder materials (McConn et al., 2011).

Material	Element	Element Weight Fraction	Isotope	Isotope Weight Fraction (Calculated)
Aluminum alloy-6061 (AA6061)	Mg	0.01	24	0.007899
			25	0.001
			26	0.001101
	Al	0.972	27	0.972
	Si	0.006	28	0.0055338
			29	0.0002802
			30	0.000186
	Ti	0.00088	46	0.0000704
			47	0.00006424
			48	0.00064944
			49	0.0000484
			50	0.00004752
	Cr	0.00195	50	8.47275E-05
			52	0.001633886
			53	0.00018527
			54	4.61175E-05
	Mn	0.00088	55	0.00088
	Fe	0.00408	54	0.00023664
			56	0.003742176
			57	0.00008976
			58	0.000011424
	Cu	0.00275	63	0.001902175
			65	0.000847825
	Zn	0.00146	64	0.00070956
			66	0.00040734
			67	0.00005986
			68	0.00027448
			70	0.00000876
Stainless Steel 316 (SS316)	C	0.00041	12	0.000405
			13	4.51E-06
	Si	0.00507	28	0.004676
			29	0.000237
			30	0.000157
	P	0.00023	31	0.00023
	S	0.00015	32	0.000143
			33	1.13E-06
			34	6.32E-06
			36	3E-08
	Cr	0.17	50	0.007387
			52	0.142441
			53	0.016152
			54	0.004021
	Mn	0.01014	55	0.01014
	Fe	0.669	54	0.038802
			56	0.613607
			57	0.014718
			58	0.001873
	Ni	0.12	58	0.081692
			60	0.031468
			61	0.001368
			62	0.004361
			64	0.001111
	Mo	0.025	92	0.00371
			94	0.002313
			95	0.00398
			96	0.00417
			97	0.002388
			98	0.006033
			100	0.002408

respectively. For these photon energies, the mass energy-absorption coefficients of Ge are 0.023 and 0.02 $cm^2.g^{-1}$,

Table 4: The average dose rate at a distance of 50 cm away from the larger surface of the sample.

Sample	Method	Decay-Delay Period (Day)					
		1	2	3	4	5	6
AA6061	RDS-31 - 0.14 (μSv.h^{-1})	15.805.5	3.661.3	1.120.5	0.350.1	0.130.05	0.060.001
	Calculation (μSv.h^{-1})	11.54	2.86	0.93	0.32	0.12	0.06
	Difference (%)	37	28	20	10	5	2
SS316	RDS-31 - 0.14 (μSv.h^{-1})	117.1920.2	10.284.3	9.283.2	8.072.7	7.332.1	6.661.8
	Calculation (μSv.h^{-1})	86.81	7.91	7.42	7.02	6.67	6.34
	Difference (%)	35	30	25	15	10	5

Table 5: Some irradiated holder properties (left) and the calculated gamma dose rates (Sv.h^{-1}) on the surface of symmetrical shielding in the transportation day (right)

Holder material	Average neutron (0-0.625 eV) flux in the D6 channel after holder batch loading (n.cm^{-2}.s^{-1})	Total mini plates inventory of Mo-99 in 6th day (Ci)	Lead shield thickness of the symmetrical container (cm)		10	15	20
AA6061	4.75E13	1700	Dose rate (μSv.h^{-1})	AA6061	1.86	8.65E-2	6.44E-3
SS316	3.36E13	1266		SS316	1.43	5.77E-2	4.39E-3

Table 6: The calculated gamma dose rates (Sv.h^{-1}) on the surface of the empty activated holder device in terms of various delay-decay times.

Holder material	Day after irradiation										
	1	2	30	60	90	180	360	540	720	900	1080
AA6061	21.2	6.8	0.11	0.08	0.06	0.04	0.02	0.013	0.008	0.005	0.002
SS316	58.2	47.8	24.6	16.3	11.3	4.4	1	0.4	0.2	0.14	0.1

respectively. Also, the mass attenuation coefficients of Be window at these energies are 0.048 and 0.033 cm^2.g^{-1}, respectively. Therefore, it can be estimated that the real ratio of photopeak areas is approximately equal to one, similar to the theoretical ratio. The unfolding spectrum based on the attenuation effect of Be and the absorption effect of Ge shows that the measured gamma spectrum is appropriately compatible with the calculated gamma lines spectrum. The experimental results verified the proposed method for the calculation of gamma spectrum and corresponding dose rate. So this method can be used to estimate the gamma dose rate which will be useful for holder device handling.

As can be seen in Table 5-left, the average flux of 0-0.625 eV neutrons at the mini-plates positions, after loading the AA6061 holder batch is about 41% more than the SS316 one. The activity of Mo-99 in all ten mini plates in the AA6061 holder batch irradiation is 34% higher than the SS316 one. Since the maximum dose rate at any point on the external surface of the transport container shall not exceed 2 mSv.h^{-1} (Agency, 2009), both holders must be transported by a container with about 22 cm lead walls. It should be noted that the depleted uranium metal is better for shielding theoretically and could reduce the container's volume.

It can be concluded that the irradiated AA6061 holder should be held in a suitable place for more than 3 years if an unexpected accident occurred and the facility was shut down. The storing time of the SS316 holder device is more. It should be noted that although the SS316 dose rate is higher, its storage room needs a thinner Pb wall at first due to lower gamma energies emitted from its inventory. But after a few days, the gamma dose rate of the AA6061 holder decreases sharply and its storage room shielding can be done with thinner Pb.

7 Conclusions

In Iran, Mo-99 demand is estimated at about 100 Ci (6 days) per week. For local production, a holder device is used to load ten fresh mini plates in the D6 channel of the TRR core. The holder batch is irradiated for 6 days at 5 MW power and then it is cooled in the reactor pool for 1 day. Then, the holder batch is transferred to the HCs to start the radiochemical process for Mo-99 production. In this paper, the radioactivity of two activated holders made of AA6061 and SS316 was investigated. For this purpose, a calculation method was proposed to estimate the delayed gamma line spectrum of the activated holder based on its isotope inventory at the time t and calculate related gamma dose rate in the different conditions. The proposed method was validated by laboratory studies on the sample plates of two selected materials and after verification, this method was used to estimate the holder dose rate and handle it. In the Research Reactors, heat is a nuisance product. Hence, the most favored for RRs are structural materials that create the least heat and/or conduct it away from the fastest. The materials with high cross-sections for neutron absorption and scattering increase heat production. They also reduce reactor efficiency by stealing neutrons from participation in fission processes. Comparison of average neutron flux in the mini-

plates positions and Mo-99 activity after 6 days irradiation shows that the AA6061 holder device is more appropriate. Furthermore, the heat removal rate is larger with higher thermal conductivity. Therefore, construction materials with low density, high specific heat, and high thermal conductivity offer the best prospects for minimizing heat generation and maximizing heat removal. In this regard, AA6061 is outstanding, too. It is also ductile, plentiful, cheap, castable, machinable, and weldable. Another attractive feature is that the activated AA6061 holder has long-lived radioisotopes less than the activated SS316 one. The transportation of the AA6061 holder batch could be done with a suitable symmetrical container with about 22 cm lead walls. When the facility must be shut down due to an accident, the shielding of its storage room needs thinner lead walls. In our future research, we intend to concentrate on managing radioactive gaseous which is produced in the dissolution process. In this case, the delay-decay period for radioactive gaseous which is accumulated in a sealed reservoir must be calculated carefully so that they can be safely released into the environment.

Conflict of Interest

The authors declare no potential conflict of interest regarding the publication of this work.

References

Abedi, E., Ebrahimkhani, M., Davari, A., et al. (2016). Neutronic and thermal-hydraulic analysis of fission molybdenum-99 production at Tehran Research Reactor using LEU plate targets. *Applied Radiation and Isotopes*, 118:160–166.

Agency, I. A. E. (2009). *Regulations for the safe transport of radioactive material*. International Atomic Energy Agency.

De Stefano, R., Pérot, B., Carasco, C., et al. (2020). Simulation of delayed gamma rays from neutron-induced fissions using MCNP 6.1. In *EPJ Web of Conferences*, volume 225, page 06007. EDP Sciences.

Domingos, D., Silva, A., Silva, J., et al. (2011). Neutronic analysis for production of fission molybdenum-99 at IEA-R1 and RMB research reactors. *RRFM 2011*.

Hasan, S. and Prelas, M. A. (2020). Molybdenum-99 production pathways and the sorbents for ^{99}Mo/^{99n}Tc generator systems using (n, γ) ^{99}Mo: a review. *SN Applied Sciences*, 2(11):1782.

Hedayat, A., Emami, J., and Salartash, R. (2021). Determination of the neutron and gamma ray dose rates of the irradiating beam tubes of a pool-type research reactor by using Monte Carlo simulation and experimental detectors regarding radiation protection issues. *International Journal of Advanced Nuclear Reactor Design and Technology*, 3:27–43.

Lee, S.-K., Beyer, G. J., and Lee, J. S. (2016). Development of industrial-scale fission ^{99}Mo production process using low enriched uranium target. *Nuclear Engineering and Technology*, 48(3):613–623.

Lee, S.-K., Lee, S., Kang, M., et al. (2020). Development of fission ^{99}Mo production process using HANARO. *Nuclear Engineering and Technology*, 52(7):1517–1523.

Lou, T. P. and Ludewigt, B. (2015). MMAPDNG: A new, fast code backed by a memory-mapped database for simulating delayed γ-ray emission with MCNPX package. *Computer Physics Communications*, 194:10–17.

McConn, R. J., Gesh, C. J., Pagh, R. T., et al. (2011). Compendium of material composition data for radiation transport modeling. Technical report, Pacific Northwest National Lab.(PNNL), Richland, WA (United States).

McKinney, G. et al. (2007). MCNPX 2.6 x features (2006-2007). Technical report, LA-UR-07-2053. Los Alamos National Laboratory.

Muenze, R., Beyer, G. J., Ross, R., et al. (2013). The Fission-Based ^{99}Mo Production Process ROMOL-99 and Its Application to PINSTECH Islamabad. *Science and Technology of Nuclear Installations*, 2013(1):932546.

Park, J. H., Choung, W., Lee, K. I., et al. (2000). Development of fission Mo-99 production technology.

To cite this article:

Miremad, S. M. , Bahrami-Samani, A. , Tabasi, M. and Ghannadi-Maragheh, M. (2025). Dosimetry and analysis of the delayed gamma rays emitted from the irradiated holder device used in Mo-99 production facilities. *Radiation Physics and Engineering*, 6(3), 1-8. doi: 10.22034/rpe.2024.475273.1238

DOI: 10.22034/rpe.2024.475273.1238

To link to this article: https://doi.org/10.22034/rpe.2024.475273.1238